

## Analysis of hydrometeorological variables over the transboundary Komadugu-Yobe basin, West Africa

O. E. Adeyeri, Patrick Laux, A. E. Lawin, S. O. Ige, Harald Kunstmann

### Angaben zur Veröffentlichung / Publication details:

Adeyeri, O. E., Patrick Laux, A. E. Lawin, S. O. Ige, and Harald Kunstmann. 2020. "Analysis of hydrometeorological variables over the transboundary Komadugu-Yobe basin, West Africa." *Journal of Water and Climate Change* 11 (4): 1339–54.  
<https://doi.org/10.2166/wcc.2019.283>.

# Analysis of hydrometeorological variables over the transboundary Komadugu-Yobe basin, West Africa

O. E. Adeyeri, P. Laux, A. E. Lawin, S. O. Ige and H. Kunstmann

## ABSTRACT

Spatiotemporal trends in daily observed precipitation, river discharge, maximum and minimum temperature data were investigated between 1971 and 2013 in the Komadugu-Yobe basin. Significant change points in time series are corrected using Adapted Caussinus-Mestre Algorithm for homogenizing Networks of Temperature series algorithm. Mann-Kendall test and Sen's slope are used to estimate the trend and its magnitude at dry, wet and annual season time scales, respectively. Preliminary results show an increasing trend of the observed variables. There is a latitudinal increase (decrease) in the basin temperature (precipitation) from lower to higher latitudes. The minimum temperature ( $0.05^{\circ}\text{C}/\text{year}$ ) increases faster than the maximum temperature ( $0.03^{\circ}\text{C}/\text{year}$ ). Overall, the percentage changes in minimum temperature range between 3 and 10% while that of maximum temperature ranges between 1 and 3%. Due to precipitation dependence on regional characteristics, the highest percentage change was recorded in precipitation with values between -5 and 97%. In all time scales, river discharge and precipitation have strong positive correlations while the correlation between river discharge and temperature is negative. It is imperative to advocate and support positive developmental practices as well as establishing necessary mitigation measures to cope with the effects of climate in the basin.

**Key words** | homogeneity tests in hydrometeorological variables, Komadugu-Yobe basin, Lake Chad region, return period, trends in hydrometeorological variables, wavelet

**O. E. Adeyeri** (corresponding author)  
West African Science Service Centre on Climate Change and Adapted Land Use,  
University of Abomey-Calavi,  
Cotonou,  
Benin  
E-mail: cyndyfem@gmail.com

**O. E. Adeyeri**  
**P. Laux**  
**H. Kunstmann**  
Institute for Meteorology and Climate Research  
Atmospheric Environmental Research,  
Karlsruhe Institute of Technology, Campus Alpine,  
Garmisch-Partenkirchen,  
Germany

**A. E. Lawin**  
Laboratory of Applied Hydrology,  
National Water Institute,  
University of Abomey-Calavi,  
Cotonou,  
Benin

**S. O. Ige**  
Nigerian Meteorological Agency,  
National Weather Forecasting and Climate  
Research Centre,  
Lagos,  
Nigeria

**H. Kunstmann**  
University of Augsburg, Institute of Geography,  
Augsburg,  
Germany

## INTRODUCTION

The effects of global warming and climate change on the environment cannot be underemphasized. This has generated considerable interest among scientists and has resulted in various studies in climate trend detection at regional (Khaliwada *et al.* 2016 in the Nepal Himalaya) and global scales (Trenberth & Shea 2005). Global climate warming is principally attributed to the significant rise in air temperature (IPCC 2013). As a result of increasing temperature, the intensity and frequency of extreme climate events such as drought

and flood are likely to increase (IPCC 2013). This could induce extreme hydrological events such as extreme river discharge, thereby affecting the hydrological cycle.

For the California drought (2012–2014), Mao *et al.* (2015) reported that warmer temperatures greatly influence river discharge while Williams *et al.* (2015) stated that increasing temperature escalates drought conditions. Over the Colorado basin, Vano *et al.* (2012) reported that warmer temperatures reduce the discharge from the Colorado River. Conversely, Reynolds *et al.* (2015) reported that the drying frequencies of intermittent streams in that basin are caused by changes occurring in both temperature and precipitation.

This is an Open Access article distributed under the terms of the Creative Commons Attribution Licence (CC BY 4.0), which permits copying, adaptation and redistribution, provided the original work is properly cited (<http://creativecommons.org/licenses/by/4.0/>).

doi: 10.2166/wcc.2019.283

At a regional scale, significant correlations have been observed between monthly mean temperature and precipitation in Europe and North America (Madden & Williams 1978). This relationship has been extended on a global scale which establishes that high maximum temperatures are accompanied by dry conditions (Trenberth & Shea 2005). Results from Trenberth & Shea (2005) showed a positive correlation between lower temperatures and higher precipitation over the continents in warm seasons. Rusticucci & Penalba (2000) established a positive correlation between warm summers and low precipitation in the north-eastern and central-western parts of Argentina, Paraguay and southern Chile. They further emphasized that cold seasons (June, July and August) exhibit a weak correlation between the variables. Furthermore, they reported a significant and positive correlation between precipitation and temperature in the coastal parts of Chile, especially between May and September as a result of high sea surface temperature which favours convection. Nicholls (2004) reported increased potential evaporation as a result of higher mean values of maximum and minimum temperatures, thereby enhancing the severity of the 2002 Australian drought.

The effect of changes in a basin's precipitation and temperature can often be related to river discharge. However, uncertainties in the trends of hydrometeorological variables as a result of data's temporal limitations, gaps in spatial coverage, change points in the dataset, regional differences and forcing cannot be down-sized (Huntington 2005). For example, after the 1976–1977 climate shift caused by the El-Nino southern oscillation (ENSO), major African rivers have experienced lower river discharges (IPCC 2013).

Attogouinon *et al.* (2017) attributed the increase in the frequency of flood events in many African countries to climate change. Over Ghana, Neumann *et al.* (2007) showed an increase of almost 0.3 °C/decade in the near surface temperature during both wet and dry seasons in the past three decades. Likewise, Adeyeri *et al.* (2019a) noted a significant positive trend in annual total rainfall, number of consecutive dry days, warm spell duration, warm day and warm night frequencies over the Komadugou-Yobe Basin (KYB). They also projected more frequent extreme precipitation and temperature events in the future. Adeyeri *et al.*

(2019b) observed an increasing trend in annual precipitation and river discharge over the KYB between 1971 and 2013. Oyebande (2001) attributed the disruption of the Jama'are and Hadejia river flow of the KYB between 1979 and 1989 to human activities, droughts and evapotranspiration losses, while Adeyeri *et al.* (2019b) showed that approximately 50% rainfall variability and 50% human activities caused an increase in discharge between 1971 and 2013.

However, the spatiotemporal behaviour of precipitation, river discharge, minimum and maximum temperature depend on the regional and local forcing. In order to proffer solutions to the problems associated with water resources management within the KYB, there is a need to understand the relationship between these variables at the basin's scale.

Therefore, this study seeks to improve the understanding of the relationships in the observed trends of precipitation, maximum air temperature, minimum air temperature and river discharge over the KYB between 1971 and 2013. Our approaches include the detection and correction of inhomogeneity in the hydrometeorological variables, trend analyses at both temporal (monthly, seasonal and annual) and spatial scales, correlation and wavelet analyses among the variables.

## STUDY AREA AND DATA USED

The KYB is situated to the south of the Sahara Desert in the Sahelian region of Africa. The elevation of the basin is between 285 and 1,750 m. It has an area cover of 150,000 km<sup>2</sup> (Figure 1) which is nearly 35% of the conventional Lake Chad basin. It is drained by the Hadejia and Jama'are rivers (Oyebande 2001). The most prominent water losses in the rivers are by infiltration, but other losses include evaporation and water abstraction (Legros 2009). The average rain season is between May and October. The mean annual precipitation ranges between 300 and 1,200 mm while the mean annual temperature is 29 °C. The climate system in this basin is governed by two main wind systems; the dry season's northeasterly wind which brings sand-dust from the Sahara Desert and the rain season's southeasterly wind which brings moisture from the Atlantic Ocean (Warner 2014). The average annual potential evaporation in the basin ranges between 1,800 mm and

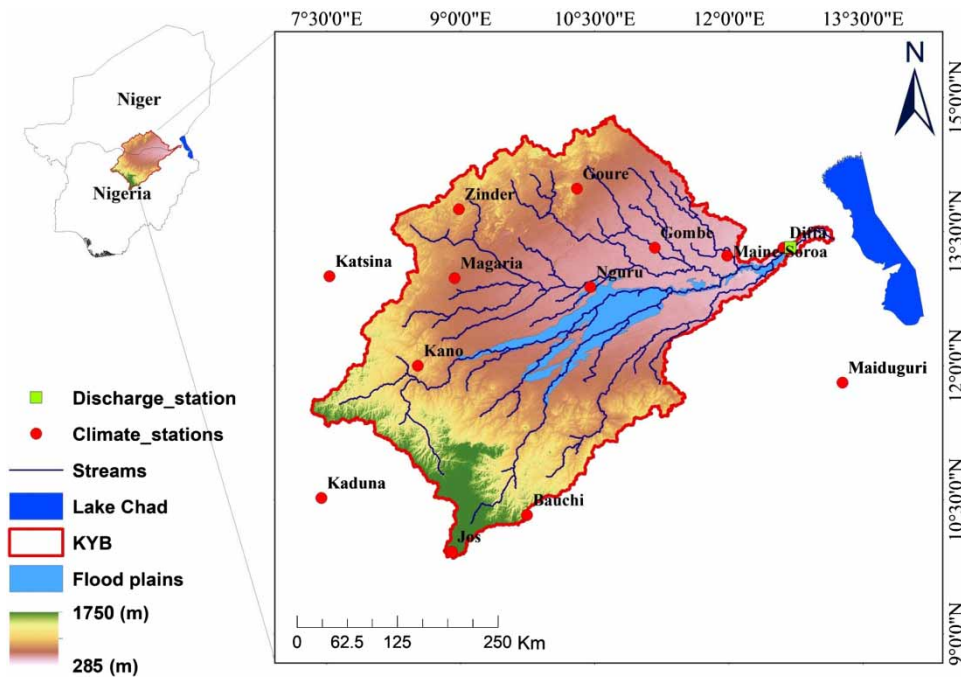


**Figure 1** | Map of the study area.

2,400 mm. The basin is characterized by the occurrences of severe drought episodes as well as high climate variability (Thompson & Polet 2000). The KYB is of strategic importance to both national and international communities because of its valuable wetlands. Additionally, some internationally shared waters originate from these wetlands. Besides its contribution to the national and international economy in terms of environmental conservation and agricultural produce, proper management of the basin strengthens the diplomatic relationships among the different countries sharing the Lake Chad Basin (IUCN 2011).

Daily precipitation, river discharge, minimum and maximum temperature data series archived by the Nigeria Meteorological Agency (NiMet), Direction de la Météorologie Nationale (DMN) of the Niger Republic and Diffa hydrological station are used for the analysis in this study (Table 1). The period of analysis for this study is between 1971 and 2013.

## METHODS

The daily climatological time series are quality controlled using the Rclimindex package (Zhang & Yang 2004).

**Table 1** | List of assimilated climatic stations

s/n	Country	Station	Lat	Long	Data range
1	Niger	Diffa	13.31	12.61	1979–2013
2	Niger	Goure	13.98	10.3	1979–2013
3	Niger	Zinder	13.75	8.98	1971–2013
4	Niger	Magaria	12.98	8.93	1979–2013
5	Niger	Maine-Soroa	13.23	11.98	1971–2013
6	Nigeria	Maiduguri	11.81	13.27	1971–2013
7	Nigeria	Potiskum	11.86	10.77	1979–2013
8	Nigeria	Katsina	13	7.53	1971–2013
9	Nigeria	Kaduna	10.52	7.44	1971–2013
10	Nigeria	Kano	12	8.52	1971–2013
11	Nigeria	Gombe	13.32	11.17	1972–2013
12	Nigeria	Nguru	12.88	10.45	1971–2013
13	Nigeria	Bauchi	10.28	9.7	1971–2013
14	Nigeria	Jos	9.92	8.9	1971–2013

During quality control, outliers and negative precipitation values and days with minimum temperature greater than maximum temperature are checked. Missing values from one station's data series (candidate series) are filled by calculating the weighted average of the other network

data series' anomalies (partner series) which are later adjusted to the candidate series' climatic mean (Domonkos & Coll 2017). There are no missing data after quality control. For a reliable and consistent climate variability and climate impact study, observational data should be checked and corrected for inhomogeneity (Acquaotta & Fratianni 2014). The Adapted Caussinus-Mestre Algorithm for homogenizing Networks of Temperature series (ACMANT) is used to check and correct the inhomogeneities in the quality controlled time series. A full description of ACMANT set up can be found in Domonkos & Coll (2017). Several studies (e.g., Domonkos & Coll 2017; Adeyeri et al. 2019a) have effectively used ACMANT in homogenizing series. The result evaluation from these studies showed good performances of homogenizing climate series with ACMANT.

The Mann-Kendall (MK) trend test (Khatiwada et al. 2016) and wavelet spectral methods (Veleda et al. 2012) are used in detecting the trend in the time series. The magnitude of the trend is estimated using the Theil and Sen's slope estimator (Khatiwada et al. 2016). The spatial trend is represented using the inverse distance weighted interpolation technique. Precipitation and discharge event return period follows the generalized extreme value (GEV) distribution function (Gilleland & Katz 2011). The GEV encompasses three types of extreme value distributions, namely, the Gumbel, Frechet and the reverse Weibull distributions. Its advantage lies in its ability to model maxima over large blocks of a data series (Gilleland & Katz 2011).

### Change points detection, step function fitting and homogenization of data series

The Caussinus Lyazrhi criterion (Caussinus & Lyazrhi 1997) and the optimal step function fitting (Domonkos & Coll 2017) are used in ACMANT to optimize break numbers in data series while the break detection incorporates the weighted reference data. The optimal step function minimizes the variance of internal distances and maximizing the variance of external distances (Adeyeri et al. 2019a). The bivariate detection method is used to identify the shifts in annual means (Domonkos & Coll 2017).

To identify the shifts in annual mean:

$$\min_{[j_1, j_2, \dots, j_k]} \left\{ \sum_{k=0}^k \sum_{i=j_k+1}^{j_{k+1}} (d(U_1)_{k,i}^2 + c(d(U)_{k,i})^2) \right\} \quad (1)$$

The internal distance ( $d$ ) is given as:

$$d(U)_i = U_{(q)i} - \overline{U_{(q)k}} \text{ where } i \in K \quad (2)$$

where  $U$  is the operator for generating of time averages,  $K$  is the total number of breaks,  $j_1$  and  $j_2$  is the starting and ending year,  $k$  is the serial number of break/step,  $q$  is the relative time series,  $i$  is the time point,  $j$  is the year,  $c$  is the empirical constant = 0.2.

To correct the inhomogeneity in data series:

$$HY_{sj} = \begin{cases} \min \text{ if } \text{sign}(t_{s,j,x}) = g \text{ for every } x \\ x = \{1, N'_{sj}\}^{[t_{s,j,x}]} \\ 0 \text{ if } \text{sign}(t_{s,j,x}) \neq g \text{ for any } x \in \{1, N'_{sj}\} \end{cases} \quad \begin{matrix} g = 1 \text{ or } g = -1 \end{matrix} \quad (3)$$

where  $HY$  is the adjustment term,  $s$  is the reference series serial number,  $x$  is an ensemble homogenization serial number,  $N'$  is the total number of usable reference series at a particular step,  $j$  is the year,  $g$  is a parameter. The details of this method are documented in Domonkos & Coll (2017).

### Trend in data series

The trend in the homogenized data series is detected by MK trend test and the wavelet spectral (Veleda et al. 2012). The MK statistic is given as (Khatiwada et al. 2016; Adeyeri et al. 2017a):

$$S = \sum_{k=1}^{n-1} \sum_{j=k+1}^n \text{Sgn}(x_j - x_k) \quad (4)$$

where  $x_j$  and  $x_k$  are sequential data values for the time series data of length  $n$ . The sum of the  $\text{Sgn}$  series is defined as:

$$\text{Sgn}(x_j - x_k) = \begin{cases} 1 \text{ if } x_j > x_k \\ 0 \text{ if } x_j = x_k \\ -1 \text{ if } x_j < x_k \end{cases} \quad (5)$$

The statistic  $S$  is approximately normally distributed with the mean  $E(S)$  and the variance  $V(S)$  can be computed as:

$$E(S) = 0 \quad (6)$$

$$V(S) = \frac{1}{18} \left\{ n(n-1)(2n+5) - \sum_{i=1}^n t_i[(t_i-1)(2t_i+5)] \right\} \quad (7)$$

where  $t$  is the extent of any given tie.  $t_i$  denotes the summation over all ties and is only used if the data series contain tied values. The standard normal variate  $Z$  is calculated by:

$$Z = \begin{cases} \frac{S-1}{\sqrt{V(S)}} & \text{if } S > 0 \\ 0 & \text{if } S = 0 \\ \frac{S+1}{\sqrt{V(S)}} & \text{if } S < 0 \end{cases} \quad (8)$$

Positive values of  $Z$  indicate a rising trend and negative values show a descending trend.

The wavelet spectral decomposes signals into signal and trends over a time period domain. This is presented as (Veleda et al. 2012):

$$C_x(a, \tau) = \int_{-\infty}^{+\infty} x(t) \psi_a^*(t-\tau/a) dt \quad (9)$$

where  $\psi_a^*(t) = (1/\sqrt{a}) \psi((t-\tau)/a)$ ,  $\psi^*$  is the complex conjugate,  $\psi(t)$  is the wavelet,  $x(t)$  continuous time signal,  $\tau$  is the shift in time ( $t$ ), 'a' is the scale and  $C_x(a, \tau)$  is the coefficient of wavelet transform.

### Slope test

Theil-Sen's estimator estimates the slope of  $n$  pairs of data points (Khaliwada et al. 2016). The magnitude of the trend is calculated as:

$$Q_i = \frac{(x_j - x_k)}{(j - k)} \text{ for } i = 1, \dots, N \quad (10)$$

where  $x_j$  and  $x_k$  are values at times  $j$  and  $k$ , respectively. Note,  $j > k$ .  $Q_i$  is a Sen's estimator of the slope which is

the median of these  $N$  values. If there are  $n$  values of  $x_j$  present in each time period, then:

$$N = n(n-2)/2 \quad (11)$$

where  $n$  is the number of time periods. The  $N$  values of  $Q_i$  are ranked by  $Q_1 \leq Q_2 \leq \dots \leq Q_{N-1} \leq Q_N$  and

$$\text{Sen's estimator} = \begin{cases} Q_{(R+1)/2} & \text{if } R \text{ is odd} \\ (1/2)(Q_{R/2} + Q_{(R+2)/2}) & \text{if } R \text{ is even} \end{cases} \quad (12)$$

The percentage change is computed by approximating it with a linear trend (Yue & Hashino 2003):

$$\text{Percentage change}(\%) = \frac{m \times l}{q} \times 100 \quad (13)$$

where  $m$  is the median slope,  $l$  is the length of the year and  $q$  is the mean of data series.

## RESULTS

### Change point detection

Table 2 shows the significant change points in precipitation, maximum and minimum temperature, respectively. In Table 2(a), significant change points are located in the precipitation series of Goure in 1999 and Potiskum station in 1994 and 1998, respectively. The other stations have homogenous data series. The maximum temperature time series (Table 2(b)) are inhomogeneous for all stations while 13 stations (except Diffa) are inhomogeneous for minimum temperature time series (Table 2(c)). These change points may be a result of changes in instruments, changes in station location and environment, station network density and structure as well as observation methods (Klein Tank et al. 2009). Other factors may include anthropogenic activities and changes in land use land cover (Adeyeri et al. 2017b; Ige et al. 2017). However, for robust analysis, these change points are corrected using the ACMANT algorithm before further analyses.



**Table 2** | Change points in data time series at 5% significant level

s/n	Stations	Year	Month	Day	Change in mean
<b>(a) Change points in daily precipitation time series</b>					
1	Goure	1999	2	31	1.2
2	Potiskum	1994	5	12	0.9
3		1998	10	16	1.6
<b>(b) Change points in daily maximum temperature time series</b>					
1	Bauchi	1984	10	31	0.4
2		2012	12	1	-1.4
3	Diffa	1990	7	31	1.2
4	Gombe	1985	3	31	0.4
5		1994	7	31	0.6
6		1998	9	30	-0.8
7		2011	3	31	-0.7
8	Goure	2005	11	30	-1.0
9	Jos	2005	11	30	-2.2
10		2006	4	30	1.9
11	Kaduna	1976	12	31	0.5
12	Kano	1983	11	30	-0.2
13	Katsina	1976	9	30	-0.3
14		1982	8	31	0.3
15	Magaria	2006	1	7	-1.4
16		2008	9	2	-0.7
17		2013	1	11	1.8
18	Maiduguri	2006	7	31	0.9
19		2007	8	31	-1.1
20	Maine-Soroa	1978	3	31	0.5
21		1982	6	30	-0.4
22		1999	9	30	0.5
23		2009	7	31	1.1
24		2010	12	29	-2.6
25	Nguru	2011	2	28	-0.6
26	Potiskum	2000	4	9	-2.3
27		2005	10	31	0.7
28	Zinder	1989	4	30	0.2
29		2004	3	31	-2.1
30		2007	9	30	0.7
<b>(c) Change points in daily minimum temperature time series</b>					
1	Bauchi	1978	1	31	0.3
2		2003	4	30	1.0
3		2007	1	31	-1.6
4		2007	11	30	1.4

(continued)

**Table 2** | continued

s/n	Stations	Year	Month	Day	Change in mean
5	Gombe	2000	12	31	2.6
6		2009	3	31	-0.6
7	Goure	1992	12	31	-1.0
8		1994	6	30	1.0
9	Jos	1978	2	28	-1.1
10		1984	3	31	-0.8
11	Kaduna	1984	3	6	-1.5
12		1984	11	23	1.5
13	Kano	1988	5	31	-0.7
14		1992	6	30	0.4
15		2010	10	31	-0.6
16	Katsina	1978	4	30	0.5
17		1990	12	31	-0.6
18		1993	3	17	-1.8
19		1996	12	31	1.4
20		2001	3	31	0.4
21	Magaria	1996	4	30	0.7
22		2000	11	30	-0.8
23		2005	12	31	1.8
24	Maiduguri	1982	3	31	-0.4
25		1986	3	31	-0.8
26		1989	6	30	0.5
27		2006	9	30	0.5
28	Maine-Soroa	1976	12	31	-0.5
29		1981	12	31	0.3
30		1997	7	31	0.6
31		2010	3	31	0.5
32	Nguru	1981	6	30	-0.5
33		1986	12	31	0.5
34		1998	3	31	-0.4
35		2013	6	30	-1.0
36	Potiskum	2008	3	31	-0.2
37	Zinder	2002	5	31	-1.2
38		2008	2	29	0.5

### Mean climatology

The monthly analysis of temperature variables (Figure 2) shows the monthly range of maximum and minimum temperature varies from 24 to 41 °C and 11 to 27 °C, respectively. The highest values of maximum temperature are seen from

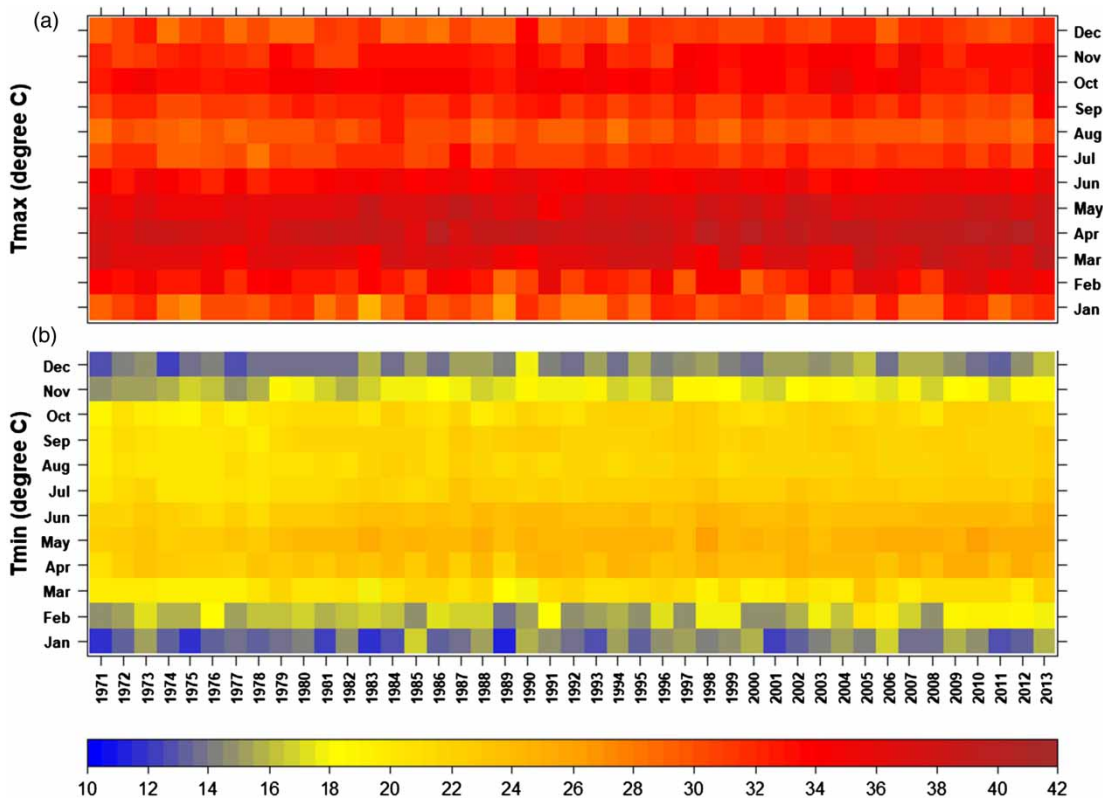


**Figure 2** | Temporal distributions of temperature variables over the KYB: (a) maximum temperature ( $^{\circ}\text{C}$ ), (b) minimum temperature ( $^{\circ}\text{C}$ ).

March to June. These months precede the significant rain months and months with high river discharge (Adeyeri *et al.* 2019b). This may be attributed to the intensification of convective precipitation at high temperatures (Berg *et al.* 2013), especially in conditions where the ocean drives the atmosphere. For minimum temperature, the highest values are seen from March to October while the lowest values are seen from December to February. Higher values of minimum temperature may be attributed to the formation of stratiform cloud in the mornings (Janiga & Thorncroft 2014). There is also a positive trend in both annual maximum and minimum temperature for the period of study (Figure 3). This temperature increase could reduce the availability of pastures to feed livestock, affect crop yield and intensify the impact of droughts (Hatfield & Prueger 2015). However, the rate of increase in minimum temperature ( $0.05^{\circ}\text{C}/\text{year}$ ) is higher than the rate of increase in maximum temperature ( $0.03^{\circ}\text{C}/\text{year}$ ). This is a pointer to more extreme hot temperature events with potential impacts on crop growth and yield (Hatfield & Prueger 2015). For example, minimum

temperature affects the respiration rates of plants during the night (Hatfield & Prueger 2011), also, high minimum temperature decreases crop yield and also enhances plants deterioration with age (Hatfield & Prueger 2015).

### Temporal and spatial trends

Table 3 presents the result of the temporal trends in discharge, temperature and rainfall time series. The monthly trend shows a non-significant decrease in the trend of discharge for all months except the months of June, July, August and September with Z values of 0.18, 0.12, 0.12 and 0.21, respectively. This was confirmed by Adeyeri *et al.* (2019b), that the river discharge in these months is between 20 and 100 mm/month while the other months have fewer discharges. The highest positive percentage of change (40%) occurs in September while the highest negative percentage of change ( $-16\%$ ) occurs in the month of March. However, for the seasonal trends, there are significantly increasing trends of discharge in both wet and



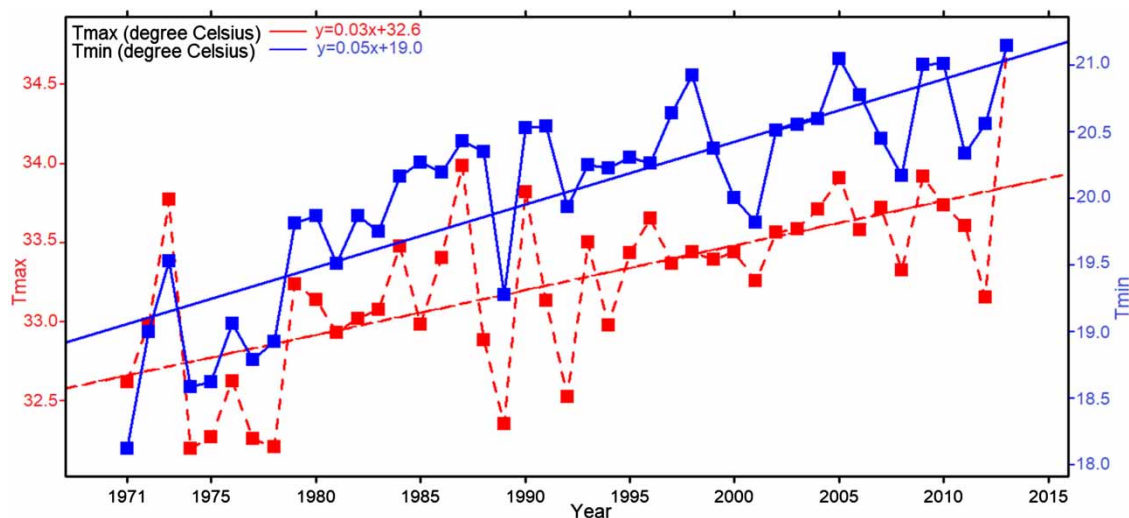


**Figure 3** | Annual trend of maximum and minimum temperature over the KYB between 1971 and 2013; x is year while y is the temperature variables.

**Table 3** | Trend in basin average discharge and precipitation for monthly, dry, wet and annual seasons

	Discharge		Precipitation		Tmax		Tmin	
	Z	%change	Z	%change	Z	%change	Z	%change
Monthly								
Jan	-0.08	-14	0.00	0	0.13	4	<b>0.23</b>	12
Feb	-0.10	-15	0.22	0	0.11	4	<b>0.23</b>	13
Mar	-0.10	-16	<b>0.30</b>	0	<b>0.24</b>	5	<b>0.24</b>	8
Apr	-0.08	-10	0.13	0	<b>0.44</b>	5	<b>0.50</b>	11
May	-0.01	-2	-0.03	0	<b>0.40</b>	6	<b>0.59</b>	11
Jun	0.18	38	-0.01	0	<b>0.30</b>	5	<b>0.58</b>	9
Jul	0.12	26	-0.15	-53	<b>0.31</b>	4	<b>0.61</b>	10
Aug	0.12	20	0.15	36	0.04	0	<b>0.54</b>	8
Sep	0.21	40	<b>0.40</b>	133	0.00	0	<b>0.45</b>	8
Oct	-0.01	-1	<b>0.44</b>	163	0.03	1	<b>0.45</b>	10
Nov	0.01	1	<b>0.41</b>	0	<b>0.32</b>	5	<b>0.40</b>	15
Dec	-0.01	-3	<b>0.28</b>	0	<b>0.22</b>	6	<b>0.32</b>	12
Seasonal								
Dry	-0.07	-11	0.37	0	0.02	4	<b>0.37</b>	10
Wet	<b>0.15</b>	26	<b>0.26</b>	47	0.21	3	<b>0.60</b>	8
Annual	<b>0.10</b>	19	<b>0.30</b>	54	<b>0.48</b>	4	<b>0.65</b>	10

Bold values represent significant trends at 5% significant level. Z is the standard normal variate indicating the trend.

annual seasons with Z values of 0.2 mm/year and 0.1 mm/year, respectively. The dry season has a non-significant decreasing Z value of -0.07 mm/year. For the precipitation time series, there is a non-significant decreasing trend in

May, June and July. However, the highest positive percentage change of 163% is recorded in October while the highest negative percentage change of -53% is recorded in July. The seasonal analysis shows an increasing trend of

rainfall for all seasons. There are increasing trends in both minimum and maximum temperature time series for all months and seasons. Nonetheless, the highest trend increase in maximum temperature is seen on the annual scale and in April with Z values of 0.5 and 0.4 °C/year, respectively. Furthermore, the highest percentage of change (6%) is seen in May. For minimum temperature, the highest increase is seen at the annual scale and in July with Z values of 0.7 and 0.6 °C/year, respectively. The highest percentage of change (15%) is seen in the month of November.

The results for the MK test in the basin show increasing trends for all variables in all stations in the KYB except Jos and Kaduna with a decreasing precipitation trend of  $-0.1$  and  $-0.05$  mm/year, respectively (Table 4). These findings agree with USGS (2012), who reported an increasing trend of temperature in the Sahel as a consequence of the warming of the northern Atlantic Ocean and the Mediterranean, thereby increasing the meridional convergence of external moisture at low levels. This eventually increases the rainfall in the region and created a partial rainfall recovery especially in the 1990s. Consequently, yearly variations in precipitation are greatly influenced by local moisture recycling rate which is controlled by planetary flow

configurations linked with the El Niño-Southern Oscillation (Sheen *et al.* 2017).

The spatial trend of the annual mean values of temperature variables in the KYB (Figure 4(a) and 4(b)) shows the range of between 34 and 35 °C in the northern part to 28 and 34 °C in the southern part for maximum temperature. The range is between 20 and 22 °C in the northern part and between 16 and 20 °C in the southern part for minimum temperature. This agrees with Funk *et al.* (2015), who observed coolest air temperatures at the southern edges of the Sahel. For results of the spatial distribution of the percentage changes in temperature for maximum temperature (Figure 4(c)), the highest percentage change (4%) is observed in Magaria while the lowest is observed in Zinder and Maine-Soroa (<2%). The highest percentage change in minimum temperature (Figure 4(d)) is observed in Jos (10%) while the lowest is observed in Goure, Magaria and Diffa (between 3% and 4%).

Highest precipitation is seen to increase towards the south-western part of the basin (Figure 5(a)). The range of precipitation in the basin is between 400 and 750 mm in the northern part to between 750 and 1,300 mm in the southern part of the basin. There is an overall latitudinal

**Table 4** | Mann-Kendall test and percentage change

Stations	Maximum temperature (Tmax)			Minimum temperature (Tmin)			Precipitation		
	Z-value	Sen's slope	% change	Z-value	Sen's slope	% change	Z-value	Sen's slope	% change
Bauchi	<b>0.23</b>	0.014	2	<b>0.44</b>	0.028	6	<b>0.3</b>	9.5	38
Diffa	<b>0.26</b>	0.03	4	0.24	0.018	4	<b>0.38</b>	4.82	69
Gombe	<b>0.36</b>	0.019	3	<b>0.42</b>	0.028	6	0.03	0.52	2
Goure	0.2	0.01	1	<b>0.25</b>	0.016	3	<b>0.47</b>	7.46	91
Jos	<b>0.44</b>	0.02	3	<b>0.54</b>	0.035	10	-0.1	-1.36	-4
Kaduna	<b>0.35</b>	0.016	2	<b>0.52</b>	0.029	7	- <b>0.05</b>	-1.26	-5
Kano	<b>0.4</b>	0.02	3	<b>0.5</b>	0.03	7	<b>0.51</b>	20.8	93
Katsina	<b>0.29</b>	0.02	3	<b>0.4</b>	0.029	6	0.17	3.63	27
Magaria	<b>0.34</b>	0.03	4	<b>0.23</b>	0.018	4	0.18	12.28	74
Maiduguri	<b>0.25</b>	0.014	2	<b>0.44</b>	0.028	6	<b>0.29</b>	5.59	42
Maine-Soroa	0.2	0.012	2	<b>0.46</b>	0.028	6	0.2	2.32	29
Nguru	<b>0.33</b>	0.02	3	<b>0.5</b>	0.029	6	0.07	1.18	12
Potiskum	0.19	0.01	1	<b>0.37</b>	0.02	4	0.58	14.69	97
Zinder	<b>0.22</b>	0.01	1	<b>0.53</b>	0.03	6	<b>0.23</b>	6.09	41

Bold value means significant trend at 5% significant level. Positive Z means increasing trend. For more information about the location of the stations, please see Figure 1.

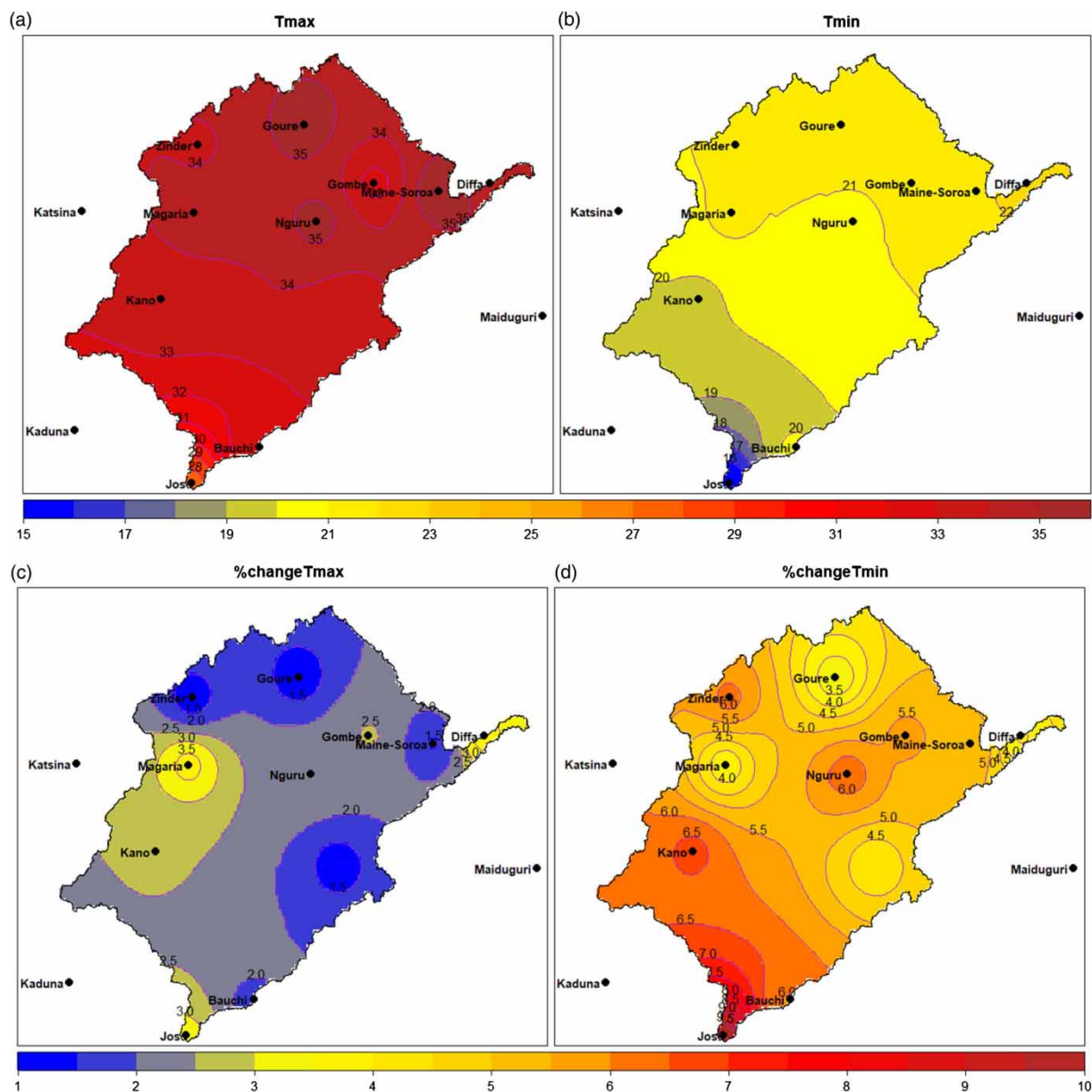


**Figure 4** | Annual temperature of the Komadugu-Yobe basin: (a) maximum air temperature (°C), (b) minimum air temperature (°C), (c) percentage change in annual maximum air temperature (%), (d) percentage change in annual minimum air temperature (%).

increase (decrease) of temperature (precipitation) i.e., from lower to higher latitudes. This is in agreement with USGS (2012).

The results of the spatial distribution of the percentage changes in precipitation are presented in Figure 5(b). The highest percentage changes in precipitation are seen in Potiskum, Kano and Goure with values between 85% and almost 100% while the lowest percentage changes are seen

in Gombe and Nguru with values between -5% and 21% (Figure 5(b)). Furthermore, the result of the periodicity in the properties of the observed variables shows different variations across different time scales (Figure 6). For example, there is an evident 3–4 years periodicity of high signal ( $\geq 4$ ) in the maximum temperature wavelet between 1971 and 1995 and between 2009 and 2013. This same high flow signal is present in minimum temperature wavelet

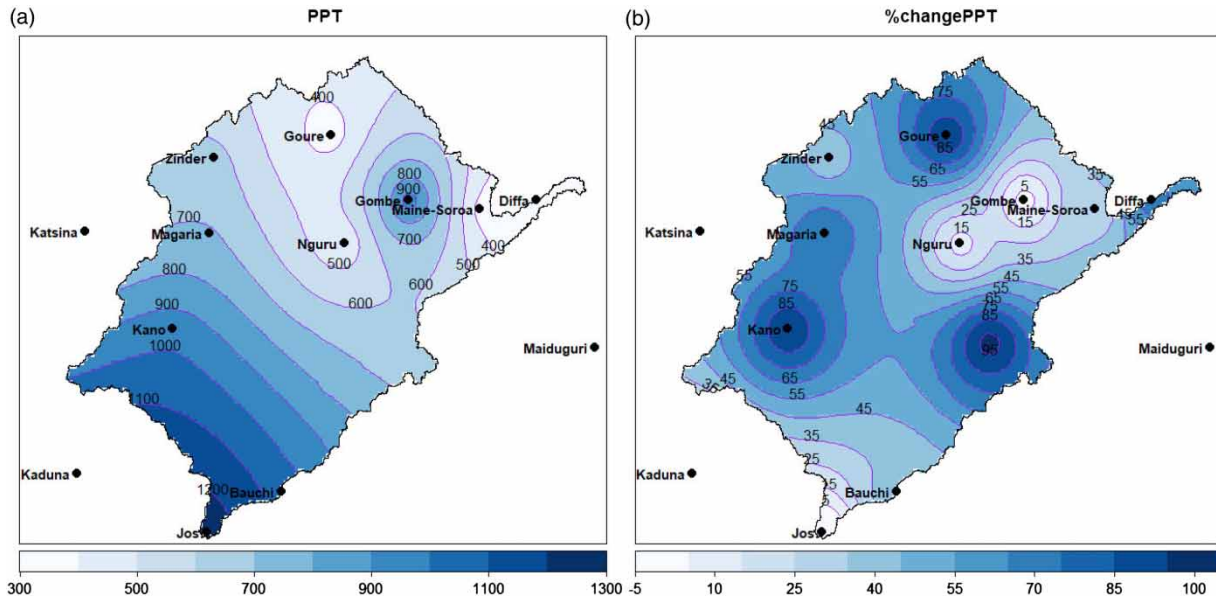


**Figure 5** | Spatial distribution of (a) annual precipitation (mm), (b) percentage change in annual precipitation (%).

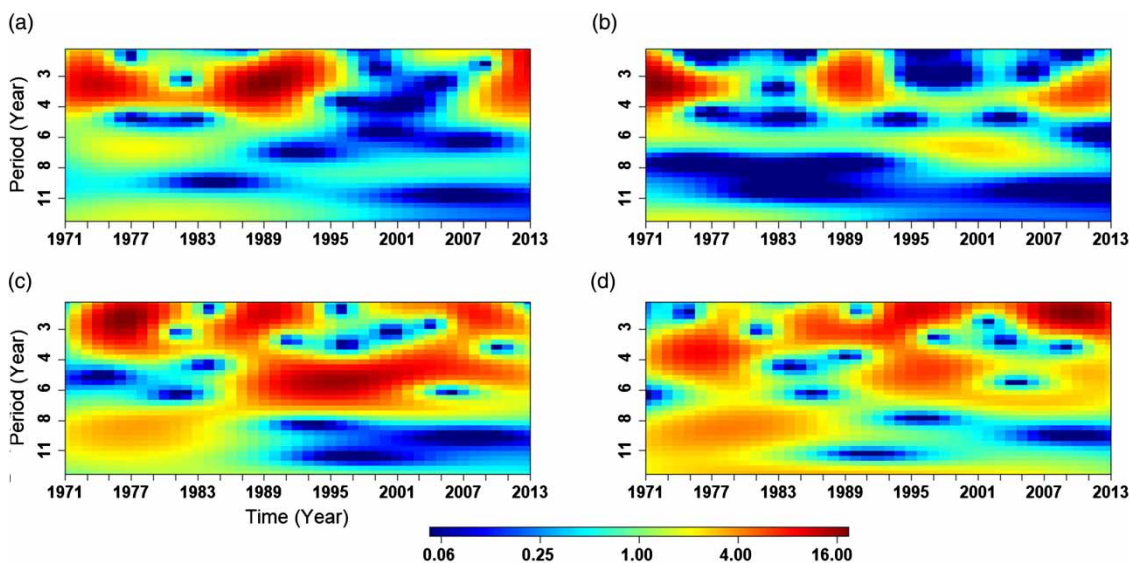


**Figure 6** | Periodicities in (a) maximum temperature (°C), (b) minimum temperature (°C), (c) precipitation (mm), (d) discharge (mm).

between 1971 and 1979, 1987 and 1995, and between 2007 and 2013. A periodicity of 8–11 years of low signals ( $\leq 0.3$ ) manifested in the minimum temperature series throughout the period of study while this is only present between 1978 and 1991 and between 1996 and 2013 for maximum temperature. However, for precipitation, there is a regular six years' periodicity of high signal ( $\geq 3$ ) between

1988 and 2013 while for discharge this same signal is captured between 1993 and 2000. Although there are some resemblances in the properties of the periodic trends of all variables which show associated trends, the dissimilarities in the pattern of trends show that the properties of the variables are being modified by non-climatic influences.

## The relationship between precipitation, temperature and river discharge

In an attempt to further understand the relationship between precipitation, river discharge, minimum and maximum temperature, the correlation plots among these variables are examined. For the dry season (Figure 7(a)), there exists a positive correlation between precipitation, minimum temperature, maximum temperature and years. Furthermore, river discharge in the dry season shows a negative correlation with the temperature variables and a decrease with years. For the wet season (Figure 7(b)), there is a negative correlation between river discharge and the two temperature variables, i.e.,  $-0.5$  for maximum temperature and  $-0.1$  for minimum temperature while the

correlation between precipitation and the maximum temperature is also seen to be negative ( $-0.3$ ).

These agree with Trenberth & Shea (2005) and Berg *et al.* (2009), who reported separately that over land in the dry season, there is a positive correlation between precipitation and temperature due to the low moisture-holding capacity of the atmosphere. Trenberth & Shea (2005) further reported that wet summers are cool, thereby creating a negative relationship between wet season maximum temperature and precipitation. In the warm season, precipitation intensity is influenced by moisture availability rather than the atmospheres' moisture storage capacity (Berg *et al.* 2009). Furthermore, the atmosphere has a higher moisture-holding capacity which reduces its rate of saturation during warmer summer. In the same vein, the local mechanism of moisture

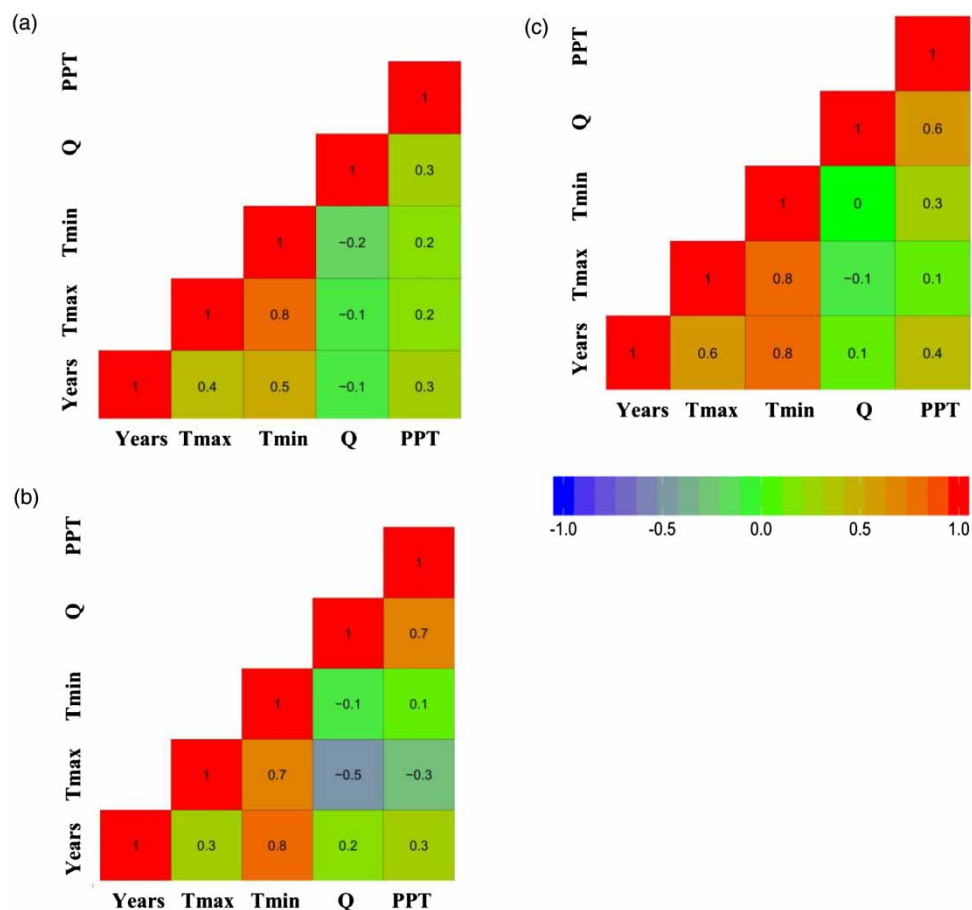


**Figure 7** | Correlation plots of basin average hydrometeorological variables using Pearson's method during: (a) dry season, (b) wet season, (c) annually. Q is the river discharge, Tmax is the maximum temperature, Tmin is the minimum temperature and PPT is the precipitation.



transport may also lower the supply of moisture during the wet season. Berg *et al.* (2009) confirmed that the process of drying soil in the wet seasons may also increase the temperatures. However, this contributory relationship is reversed in the dry months. For the annual season (Figure 7(c)), all variables show positive correlations except for the correlation between discharge and maximum temperature which is  $-0.1$  while there is no correlation between discharge and minimum temperature.

In all seasons, the river discharge and precipitation have strong positive correlations. This may be attributed to discharge increase as a result of the precipitation recovery after the drought episodes (Guo *et al.* 2014).

According to Trenberth *et al.* (2003) and Berg *et al.* (2009), heavy precipitation intensity is enhanced by increasing temperature through increased atmospheric moisture which drives the precipitation event through moisture convergence at low levels. As a consequence of the heavy precipitation intensity and discharge, there have been flooding events in the basin.

To avert flooding, farmers in the basin have been taking self-determined individual measures such as blocking and diverting of the river channels in order to minimize the loss of farms and crops (Muhammad *et al.* 2015). For

adequate preparation and planning, the frequency of flood and precipitation event occurrence is examined. Figure 8 shows that the recurrence interval of rainfall at 400 mm is 6 years while the recurrence interval of discharge higher than 30 mm is 2 years. At the upper bound, the return level of precipitation of almost 600 mm and discharge at above 50 mm is at 20 years' recurrence interval. This will provide useful information as regards flood event preparedness.

## CONCLUSION

The study investigated the inhomogeneity and analysed the spatiotemporal trends as well as the relationship between precipitation, river discharge, maximum and minimum temperature over the KYB, Lake Chad region between 1971 and 2013. Significant change points in the time series were detected and corrected using ACMANT. This correction provides a more robust time series for climate impact studies in the basin. Initial results show a latitudinal increase (decrease) in the basin temperature (precipitation) from lower to higher latitudes. There is, overall, increasing temperature, precipitation and river discharge in the basin.

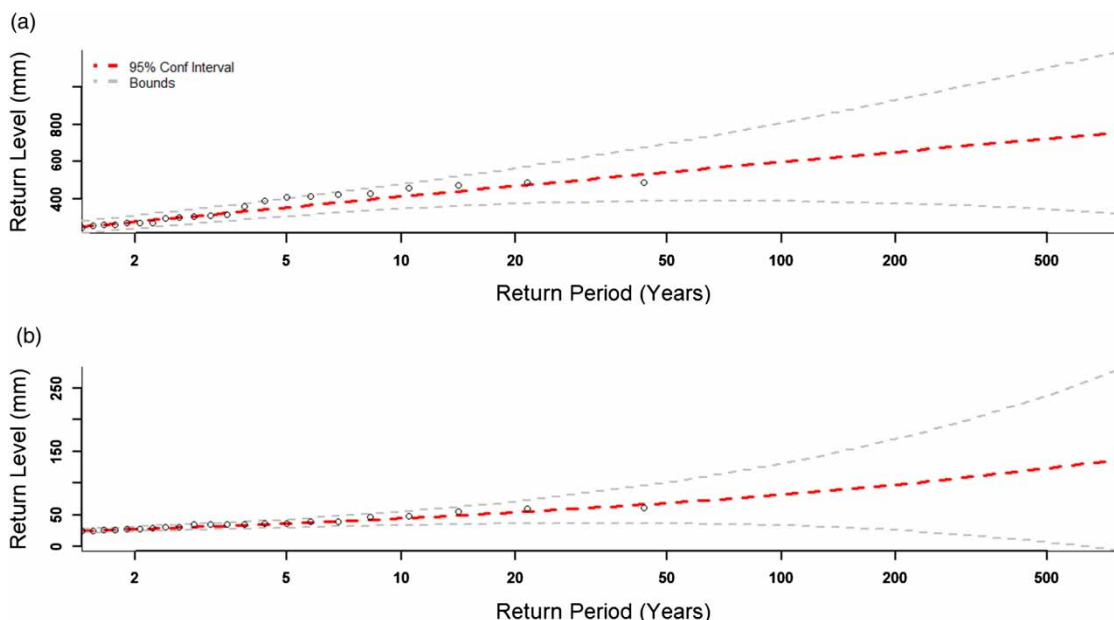


**Figure 8** | Flow return period: (a) precipitation, (b) discharge.



On the other hand, increasing rainfall as a result of the Sahelian rainfall recovery could revive the wetlands in the basin, thereby maintaining the food chain balance and preserving the ecosystem. However, excess water from heavy precipitation intensity as a result of increasing temperature as well as increasing river discharge could lead to flooding, thus, farmlands, farm produce and properties could be affected. This could have significant impacts on water management and the socio-economic activity in the basin. Furthermore, the impacts of drought on water demand and supply by natural systems and humans could be aggravated by the warming climate (Cook et al. 2015). Adequate measures and relevant developmental practices should be put in place to mitigate the warming trend as well as flooding that could arise as a result of the increased precipitation and discharge.

There should be a coordinated effort from all stakeholders in participatory dialogue in understanding and tackling climate and environmental issues in the basin. This will promote a harmonized management of climate extreme events, flood, land, water and associated resources without compromising the sustainability of dynamic ecosystems in the basin. Established transboundary cooperation should establish effective linkages between various sectors for the development of integrated water planning and management to eliminate confrontational cross-border impacts in the management of the basin.

However, in an attempt to secure the basin resources from climate extreme events, feasibility studies and environmental impact assessment should be prioritized before embarking on relevant developmental projects. Nevertheless, limited hydrological and climatic data of sufficient quality have hindered sound research and in-depth investigations of the basin's hydrology. Future works should seek to include more recent data.

## ACKNOWLEDGEMENTS

The first author was supported by a doctoral scholarship from the Federal Ministry of Education and Research (BMBF) and West African Science Service Center on Climate Change and Adapted Land Use (WASCAL). The authors wish to acknowledge the Direction de la

Météorologie Nationale (DMN) of Niger Republic, the Nigeria Meteorological Agency (NiMet) for the climate data used in this study. We also acknowledge the fruitful discussions with Seyni Salack of the WASCAL competent centre, Burkina Faso. We extend our thanks to Peter Domonkos for the provision of the ACMANT package as well as the constructive discussions regarding the use of ACMANT. The anonymous reviewers are also acknowledged. The authors have read and understood the policy on declaration of interests and declare that we have no competing interests.

## REFERENCES

- Acquaotta, F. & Fratianni, S. 2014 The importance of the quality and reliability of the historical time series for the study of climate change. *Revista Brasileira de Meteorologia* **10**, 20–38.
- Adeyeri, O. E., Lamptey, B. L., Lawin, A. E. & Sanda, I. S. 2017a Spatio-temporal precipitation trend and homogeneity analysis in Komadugu-Yobe Basin, Lake Chad region. *Journal of Climatology and Weather Forecasting* **5** (3), 1000214.
- Adeyeri, O. E., Akinsanola, A. A. & Ishola, K. A. 2017b Investigating surface urban heat island characteristics over Abuja, Nigeria: relationship between land surface temperature and multiple vegetation indices. *Remote Sensing Applications: Society and Environment* **7**, 57–68.
- Adeyeri, O. E., Lawin, A. E., Laux, P., Ishola, K. A. & Ige, S. O. 2019a Analysis of climate extreme indices over the Komadugu-Yobe basin, Lake Chad region: past and future occurrences. *Weather and Climate Extremes* **23**. <https://doi.org/10.1016/j.wace.2019.100194>
- Adeyeri, O. E., Laux, P., Lawin, A. E. & Arnault, J. 2019b Assessing the impact of human activities and rainfall variability on the river discharge of Komadugou-Yobe Basin, Lake Chad Area. *Environmental Earth Sciences* (Under review).
- Attogouinon, A., Lawin, A., M'Po, Y. & Houngue, R. 2017 Extreme precipitation indices trend assessment over the Upper Oueme River Valley-(Benin). *Hydrology* **4** (4), 36.
- Berg, P., Haerter, J. O., Thejll, P., Piani, C., Hagemann, S. & Christensen, J. H. 2009 Seasonal characteristics of the relationship between daily precipitation intensity and surface temperature. *Journal of Geophysical Research* **114** (D18), 224.
- Berg, P., Moseley, C. & Haerter, J. O. 2013 Strong increase in convective precipitation in response to higher temperatures. *Nature Geoscience* **6**, 181–185. doi:10.1038/ngeo1731.
- Caussinus, H. & Lyazrhi, F. 1997 Choosing a linear model with a random number of change-points and outliers. *Annals of the Institute of Statistical Mathematics* **49**, 761–775.

- Cook, B. I., Ault, T. R. & Smerdon, J. E. 2015 Unprecedented 21st-century drought risk in the American Southwest and Central Plains. *Science Advances* **1**, e1400082–e1400082.
- Domonkos, P. & Coll, J. 2017 Homogenisation of temperature and precipitation time series with ACMANT3: method description and efficiency tests. *International Journal of Climatology* **37**, 1910–1921.
- Funk, C., Peterson, P., Landsfeld, M., Pedreros, D., Verdin, J., Shukla, S., Husak, G., Rowland, J., Harrison, L., Hoell, A. & Michaelsen, J. 2015 The climate hazards infrared precipitation with a stations – a new environmental record for monitoring extremes. *Scientific Data* **2**, 150066.
- Gilleland, E. & Katz, R. 2011 New software to analyze how extremes change over time. *Eos* **9** (2), 13–14.
- Guo, Y., Li, Z., Amo-Boateng, M., Deng, P. & Huang, P. 2014 Quantitative assessment of the impact of climate variability and human activities on runoff changes for the upper reaches of Weihe River. *Stochastic Environmental Research and Risk Assessment* **28** (2), 333–346.
- Hatfield, J. L. & Prueger, J. H. 2011 Agroecology: Implications for plant response to climate change. In: *Crop Adaptation to Climate Change* (S. S. Yadav, R. J. Redden, J. L. Hatfield, H. Lotze-Campen & A. E. Hall eds). Wiley-Blackwell, Chichester, UK, pp. 27–43.
- Hatfield, J. L. & Prueger, J. H. 2015 Temperature extremes: effect on plant growth and development. *Weather and Climate Extremes* **10**, 4–10.
- Huntington, T. G. 2005 Evidence for intensification of the global water cycle: review and synthesis. *Journal of Hydrology* **319** (1–4), 83–95.
- Ige, S. O., Ajayi, V. O., Adeyeri, O. E. & Oyekan, K. S. A. 2017 Assessing remotely sensed temperature humidity index as human comfort indicator relative to land-use landcover change in Abuja Nigeria. *Spatial Information Research* **25**, 523–533.
- IPCC 2013 *Summary for Policymakers in Climate Change 2013: The Physical Science Basis: Working Group I Contribution to the Fifth Assessment Report of the Intergovernmental Panel on Climate Change*. Cambridge University Press, Cambridge, UK, pp. 3–29.
- IUCN 2011 Komadugu Yobe Basin, upstream of Lake Chad, Nigeria. *Multi-stakeholder participation to create new institutions and legal frameworks to manage water resources*. <https://portals.iucn.org/library/efiles/documents/2011-097.pdf> (accessed 18 August 2018).
- Janiga, M. A. & Thorncroft, C. D. 2014 Convection over tropical Africa and the East Atlantic during the West African monsoon: regional and diurnal variability. *Journal of Climate* **27**, 4159–4188.
- Khatiawada, K., Panthi, J., Shrestha, M. & Nepal, S. 2016 Hydro-climatic variability in the Karnali River Basin of Nepal Himalaya. *Climate* **4**, 17.
- Klein Tank, A. M. G., Zwiers, F. W. & Zhang, X. 2009 *Guidelines on Analysis of Extremes in A Changing Climate in Support of Informed Decisions for Adaptation*. World Meteorological Organization, Geneva, Switzerland.
- Legros, J. P. 2009 De l'École régionale d'agriculture de Montpellier à Montpellier-SupAgro et Agropolis. (From Montpellier regional school of agriculture to Montpellier-SupAgro and agropolis). *Pour* **200**, 71.
- Madden, R. A. & Williams, J. 1978 The correlation between temperature and precipitation in the United States and Europe. *Monthly Weather Review* **106**, 142–147.
- Mao, Y., Nijssen, B. & Lettenmaier, D. P. 2015 Is climate change implicated in the 2013-2014 California drought? A hydrologic perspective. *Geophysical Research Letters* **42**, 2805–2813.
- Muhammad, J. C., Yahaya, D. K. & Abba, J. G. 2015 Water Management Issues in the Hadejia Jama'are-Komadugu-Yobe Basin: DFID-JWL and stakeholders experience in information sharing, reaching consensus and physical interventions. In *Conference Papers h037511*. International Water Management Institute. <https://core.ac.uk/download/pdf/6764774.pdf>
- Neumann, R., Jung, G., Laux, P. & Kunstmann, H. 2007 Climate trends of temperature, precipitation and river discharge in the Volta Basin of West Africa. *Journal of River Basin Management* **5** (1), 17–30.
- Nicholls, N. 2004 The changing nature of Australian droughts. *Climatic Change* **63**, 323–336.
- Oyebande, L. 2001 Streamflow regime change and ecological response in the Lake Chad basin in Nigeria. *Linking Hydrology and Aquatic Ecology* **266**, 105–106.
- Reynolds, L. V., Shafroth, P. B. & LeRoy Poff, N. 2015 Modeled intermittency risk for small streams in the Upper Colorado River Basin under climate change. *Journal of Hydrology* **523**, 768–780.
- Rusticucci, M. & Penalba, O. 2000 Precipitation seasonal cycle over Southern South America. *Climate Research* **16**, 1–15.
- Sheen, K. L., Smith, D. M., Dunstone, N. J., Eade, R., Rowell, D. P. & Vellinga, M. 2017 Skilful prediction of Sahel summer rainfall on inter-annual and multi-year timescales. *Nature Communications* **8**, 14966.
- Thompson, J. R. & Polet, G. 2000 Hydrology and land use in a Sahelian floodplain wetland. *Wetlands* **20**, 639–659.
- Trenberth, K. E. & Shea, D. J. 2005 Relationships between precipitation and surface temperature. *Geophysical Research Letters* **32**, L14703.
- Trenberth, K. E., Dai, A., Rasmussen, R. M. & Parsons, D. B. 2003 The changing character of precipitation. *Bulletin of the American Meteorological Society* **84**, 1205–1217.
- USGS 2012 Famine Early Warning Systems Network-informing Climate Change Adaptation Series. A Climate Trend Analysis of Niger. *Fact Sheet 3080*. <https://pubs.usgs.gov/fs/2012/3080/fs2012-3080.pdf>
- Vano, J. A., Das, T. & Lettenmaier, D. P. 2012 Hydrologic sensitivities of Colorado River runoff to changes in precipitation and temperature. *Journal of Hydrometeorology* **13**, 932–949.
- Veleda, D., Montagne, R. & Araujo, M. 2012 Cross-wavelet bias corrected by normalizing scales. *Atmospheric Oceanic Technology* **29**, 1401–1408.

- Warner, T. T. 2014 *Desert Meteorology*. Cambridge University Press, New York, USA.
- Williams, A. P., Seager, R., Abatzoglou, J. T., Cook, B. I., Smerdon, J. E. & Cook, E. R. 2015 [Contribution of anthropogenic warming to California drought during 2012-2014](#). *Geophysical Research Letters* **42**, 6819–6828.
- Yue, S. & Hashino, M. 2003 [Long-term trends of annual and monthly precipitation in Japan](#). *Journal of the American Water Resources Association* **39**, 587–596.
- Zhang, X. & Yang, F. 2004 *RClimDex (1.0) User Manual*. Climate Research Branch Environment, Ontario, Canada. <http://etccdi.pacificclimate.org/software.shtml> (accessed 13 March 2017).

First received 6 December 2018; accepted in revised form 2 June 2019. Available online 16 July 2019